

Measurement of transverse hyperfine interaction by forbidden transitions

Mo Chen (陈墨),^{1,2,*} Masashi Hirose,^{1,3,*} and Paola Cappellaro^{1,3,†}

¹Research Laboratory of Electronics, Massachusetts Institute of Technology, Cambridge, Massachusetts 02139, USA

²Department of Mechanical Engineering, Massachusetts Institute of Technology, Cambridge, Massachusetts 02139, USA

³Department of Nuclear Science and Engineering,

Massachusetts Institute of Technology, Cambridge, Massachusetts 02139, USA

Precise characterization of a system's Hamiltonian is crucial to its high-fidelity control that would enable many quantum technologies, ranging from quantum computation to communication and sensing. In particular, non-secular parts of the Hamiltonian are usually more difficult to characterize, even if they can give rise to subtle but non-negligible effects. Here we present a strategy for the precise estimation of the transverse hyperfine coupling between an electronic and a nuclear spin, exploiting effects due to nominally forbidden transitions during the Rabi nutation of the nuclear spin. We applied the method to precisely determine the transverse coupling between a Nitrogen-Vacancy center electronic spin and its Nitrogen nuclear spin. In addition, we show how this transverse hyperfine coupling, that has been often neglected in experiments, is crucial to achieving large enhancements of the nuclear Rabi nutation rate.

Quantum technologies promise to revolutionize many fields, ranging from precision sensing to fast computation. The success of novel technologies based on quantum effects rests on engineering quantum systems robust to noise and decoherence and on controlling them with high precision. Solid-state systems comprising nuclear spins have emerged as promising candidates, since the nuclear spin qubits are only weakly coupled to external fields and thus exhibit long coherence times. In order for nuclear spins to be used as good qubits, there are two important requirements: their Hamiltonians need to be known with very high precision, as this would enable applying e.g. optimal control methods^{1,2}, and strong driving should be available, in order to achieve fast gates. Here we show how to meet these two requirements by exploiting nominally forbidden transitions in a hybrid electronic-nuclear spin system associated with the Nitrogen-Vacancy center in diamond³. Specifically, we use second-order effects due to mixing of the electronic and nuclear spin states⁴ in order to identify with high precision their coupling strength and to enhance the nuclear spin nutation rate⁵.

The nitrogen vacancy (NV) center is a naturally occurring point defect in diamond⁶. Thanks to its optical properties and long coherence times, it has emerged as a versatile system for quantum sensing⁷⁻⁹, quantum information^{10,11} and photonics applications^{12,13}. The nuclear ¹⁴N spin often plays an important role in these applications. Not only can it serve as a qubit in small quantum algorithms¹⁴⁻¹⁶, but it can also be used to enhance the readout fidelity of the NV electronic spin¹⁷ and achieve more sensitive detection of magnetic fields^{18,19} and rotations^{20,21}. These applications are made possible by the hyperfine interaction between the NV electronic and nuclear spins.

While the secular part of the NV-¹⁴N Hamiltonian has been well-characterized before²²⁻²⁴, the transverse hyperfine coupling is more difficult to measure²⁵ and published values do not match well²⁶⁻²⁸. The most precise characterization to date has been achieved by ensemble ESR techniques²⁷. In that work, the ESR spectrum of an en-

semble of NV centers was measured by induction methods while applying a magnetic field along the $\langle 110 \rangle$ direction to amplify nominally forbidden transitions. This method is not applicable to single NV centers, since the strong transverse field would quench the spin-dependent optical contrast.

Here we propose a different strategy to measure the transverse hyperfine coupling that can be carried out with optically detected magnetic resonance. Thanks to this method we can determine the value of the transverse coupling with a better precision than achieved previously. The method is not restricted to the NV spin system, but could be applied more generally to other electronic-nuclear spin systems, such as phosphorus²⁹ or antimony³⁰ donors in silicon, defects in silicon carbide^{31,32} or quantum dots³³. Precise knowledge of the hyperfine interaction tensor would enable achieving more precise control, elucidating modulations of the NV echo dynamics or, as we show here, achieving faster Rabi nutation of the nuclear spin.

Theoretical Model – The NV ground state is a two-spin system given by the electronic spin of the NV center ($S = 1$) and the nuclear spin ($I = 1$) of the substitutional ¹⁴N adjacent to the vacancy that comprise the defect. In the experiments, we are only interested in two of the nuclear spin levels ($m_I = +1, 0$) that we drive on-resonance, while the third level can be neglected. Then, the Hamiltonian of the reduced system³⁴ is given by $\mathcal{H} = \mathcal{H}_{\parallel} + \mathcal{H}_{\perp}$, where the secular, \mathcal{H}_{\parallel} , and nonsecular, \mathcal{H}_{\perp} , terms are:

$$\begin{aligned}\mathcal{H}_{\parallel} &= \Delta S_z^2 + (\gamma_e B_z + \frac{A_{\parallel}}{2}) S_z + (Q + \gamma_n B_z) I_z + A_{\parallel} S_z I_z, \\ \mathcal{H}_{\perp} &= \sqrt{2} A_{\perp} (S_x I_x + S_y I_y).\end{aligned}\tag{1}$$

Here S and I are the electron spin-1 and nuclear spin-1/2 operator respectively. $\Delta = 2.87$ GHz is the zero-field splitting and $Q = -4.945$ MHz²³ the nuclear quadrupolar interaction. The NV spin is coupled to the nuclear spin by a hyperfine interaction with a longitudinal component $A_{\parallel} = -2.162$ MHz²³ and a transverse component A_{\perp} which we want to estimate. A magnetic field

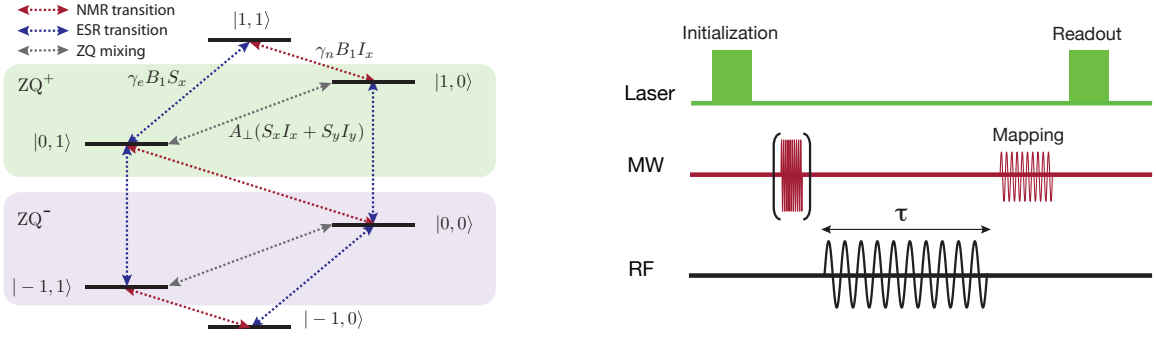


FIG. 1. Left: energy levels of the reduced NV- ^{14}N spin system, showing the transitions that are mixed by the transverse hyperfine coupling. Right: Experimental sequence used to measure the nuclear ^{14}N Rabi frequency in the three NV manifolds.

B_z is applied along the NV crystal axis [111] to lift the degeneracy of the $m_s = \pm 1$ level, yielding the electron and nuclear Zeeman frequencies $\gamma_e B_z$ and $\gamma_n B_z$ where $\gamma_e = 2.8$ MHz/G and $\gamma_n = -0.308$ kHz/G.

Let $|m_s, m_I\rangle$ be eigenstates of \mathcal{H}_{\parallel} . The transverse coupling A_{\perp} mixes states connected via zero-quantum (ZQ) transitions, $|+1, 0\rangle \leftrightarrow |0, 1\rangle$ and $|0, 0\rangle \leftrightarrow |-1, 1\rangle$. Diagonalization of the total Hamiltonian can then be achieved by rotating the two ZQ subspaces with a unitary transformation $U_{\text{ZQ}} = e^{-i(\sigma_y^- \vartheta^- + \sigma_y^+ \vartheta^+)}$, where we defined $\sigma_y^+ = i(|+1, 0\rangle\langle 0, 1| - |0, 1\rangle\langle +1, 0|)$; $\sigma_y^- = i(|0, 0\rangle\langle -1, 1| - |-1, 1\rangle\langle 0, 0|)$ and the rotation angles are

$$\begin{aligned} \tan(2\vartheta^+) &= \frac{2A_{\perp}}{\Delta + \gamma_e B_z - \gamma_n B_z - Q}, \\ \tan(2\vartheta^-) &= \frac{-2A_{\perp}}{\Delta - \gamma_e B_z - A_{\parallel} + \gamma_n B_z + Q}. \end{aligned} \quad (2)$$

Because of this level mixing, a field on resonance with the nuclear spin transition also drives electronic transitions. Although the electronic spin state is unchanged to first order, as long as the mixing is small, the nominally forbidden transitions result in an enhancement of the nuclear state nutation frequency, as we explain below.

When applying a radio frequency (RF) field to drive the nuclear spin, the interaction Hamiltonian of the NV- ^{14}N system with the RF field is:

$$\mathcal{H}_{\text{rf}}(t) = 2B_1 \cos(\omega t)(\gamma_e S_x + \sqrt{2}\gamma_n I_x), \quad (3)$$

where B_1 is the RF field strength. The Hamiltonian can be simplified by going into a rotating picture at the RF frequency ω and applying the rotating wave approximation (RWA), to obtain $\mathcal{H}_{\text{rf}} = B_1(\gamma_e S_x + \sqrt{2}\gamma_n I_x)$. We note that since we might have $\gamma_e B_1 \gg \omega$, effects from the counter-rotating fields, such as Bloch-Siegert shifts of the electronic energies, might be present. These effects were however negligible at the fields and Rabi strengths used in the experiments³⁴. Transforming \mathcal{H}_{rf} with the unitary U_{ZQ} and denoting states and operators in the new frame

by a hat, we obtain $\hat{\mathcal{H}}_{\text{rf}} = U_{\text{ZQ}} \mathcal{H}_{\text{rf}}(t) U_{\text{ZQ}}^{\dagger} = \mathcal{H}_n + \mathcal{H}_e$, with

$$\mathcal{H}_n = \sqrt{2}\gamma_n B_1 (\alpha_1 |\hat{1}\rangle\langle \hat{1}|_e + \alpha_0 |0\rangle\langle 0|_e + \alpha_{-1} |-\hat{1}\rangle\langle -\hat{1}|_e) \hat{I}_x \quad (4)$$

Here α_{m_s} denote the enhancement factors in each manifold of the NV spin:

$$\alpha_{+1} \approx 1 + \frac{\gamma_e}{\gamma_n} \frac{A_{\perp}}{\Delta + \gamma_e B_z - \gamma_n B_z - Q}, \quad (5)$$

$$\begin{aligned} \alpha_0 \approx 1 - \frac{\gamma_e}{\gamma_n} \left(\frac{A_{\perp}}{\Delta + \gamma_e B_z - \gamma_n B_z - Q} \right. \\ \left. + \frac{A_{\perp}}{\Delta - \gamma_e B_z - A_{\parallel} + \gamma_n B_z + Q} \right), \end{aligned} \quad (6)$$

$$\alpha_{-1} \approx 1 + \frac{\gamma_e}{\gamma_n} \frac{A_{\perp}}{\Delta - \gamma_e B_z - A_{\parallel} + \gamma_n B_z + Q}, \quad (7)$$

where we show expressions exact up to the first order in ϑ^{\pm} (see³⁴ for the exact expressions). The Hamiltonian \mathcal{H}_e can be neglected since electronic spin transitions are far off-resonance.

Thanks to the strong dependence of the enhancement factors on the transverse hyperfine coupling, we can determine A_{\perp} with high precision from measurement of the ^{14}N Rabi oscillations.

Experiments – We used a home-built confocal microscope to measure the transverse hyperfine interaction of a single NV center in an electronic grade diamond sample (Element 6, ^{14}N concentration $n_N < 5$ ppb, natural abundance of ^{13}C). The NV center is chosen to be free from close-by ^{13}C . We worked at magnetic fields (300-500G) close to the excited state level anti-crossing so that during optical illumination at 532nm, polarization of the NV spin can be transferred to the nuclear spin by their strong hyperfine coupling in the excited state³⁵. As a result, a $1\mu\text{s}$ laser excitation polarizes the NV- ^{14}N system into the $|0, 1\rangle$ state.

Then, the NV spin is prepared in the desired Zeeman state by a strong microwave (MW) pulse ($t_p \approx 50\text{ns}$) before coherently driving the nuclear spin by an RF field on resonance with the nuclear transition $|m_s, 1\rangle \leftrightarrow |m_s, 0\rangle$, for a duration τ (see Fig. 1). Finally, the nuclear spin

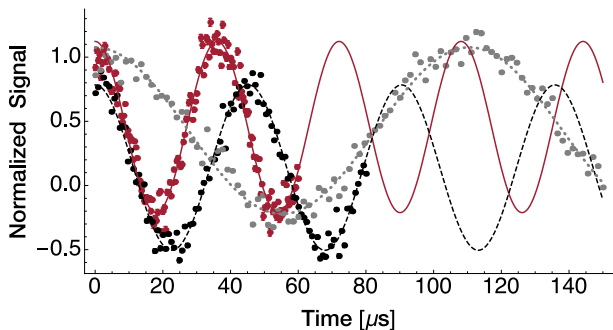


FIG. 2. ^{14}N Rabi oscillations at $B = 450\text{G}$, $B_1 \approx 3.3\text{G}$ in the three NV manifold (Red, solid line $m_s = 0$. Black, dashed line, $m_s = -1$. Gray, dotted line $m_s = +1$). Here the dots are the experimental results, while the lines are fits to cosine oscillations. The different baseline of the $m_s = -1$ curve is due to small differences in the fluorescence emission of different nuclear manifolds³⁵.

state is detected by employing a MW selective pulse ($t_p \approx 700$ ns) that maps the nuclear spin state onto the NV spin, which in turn can be read out optically due to spin-dependent fluorescence emission intensity. The nuclear Rabi oscillations in Fig. (2) clearly show that for a fixed driving strength, the effective Rabi frequency is quite different in the three electronic spin manifolds.

To confirm the expected dependence of the Rabi enhancement factors on the external magnetic field and the NV state, we measured the Rabi oscillations at the three electronic spin manifolds with varying magnetic field B_z . As shown in Fig. (3), the measured Rabi frequencies match well with the theoretical model. It is worth noting that contrary to the static pseudo-nuclear Zeeman effect⁴, there is a large enhancement ($\alpha_0 \sim 16$, $\alpha_{\pm 1} \approx -9$) even at zero field. Also, close to the ground state avoided crossing ($B \approx 0.1$ T) the enhancement can become very large, exceeding 100. The validity of our approximation in this regime can be confirmed by numerical simulations³⁴.

While these experiments could be used to extract A_{\perp} , this is not a practical method to obtain a good enough estimate. The range of magnetic field is restricted by the need to be close to the excited state level anti-crossing, to achieve a good polarization of the nuclear spin. The number of acquired points is limited by the time it takes to change and properly align the external magnetic field. In addition, there might be variations in the bare Rabi frequency in the three manifolds, because of different responses of the electronics used to drive the nuclear spins at the different frequencies.

In order to avoid these difficulties, we fixed the magnetic field to 509G and instead linearly swept the amplitude of the RF driving (B_1). With this procedure, we do not need an independent measure of the bare Rabi frequency in order to extract the transverse hyperfine coupling strength. The relative RF amplitudes B_1 obtained when varying the driving strength can be measured at

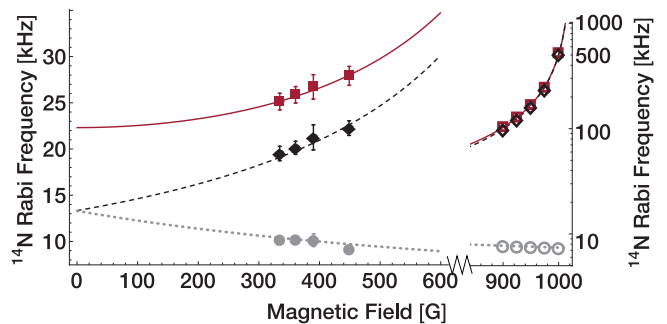


FIG. 3. ^{14}N Rabi Frequency in the three NV manifold (Red, solid line $m_s = 0$. Black, dashed line, $m_s = -1$. Gray, dotted line $m_s = +1$) as a function of the magnetic field. Rabi frequency corresponds to $\frac{\gamma_n B_1}{\sqrt{2\pi}} \alpha_{m_s}$. The filled symbols correspond to the experimental data, which matches closely the theoretical prediction. The effective Rabi frequencies increase rapidly with the field, exceeding 1 MHz when close to ground state level anti-crossing. The enhancement allows fast manipulation of the nuclear spin even when the bare Rabi field is only $B_1 \approx 3.3\text{G}$. The theoretical prediction is confirmed by simulations (open symbols) of the spin dynamics.

each nuclear resonance frequency by monitoring the RF voltage with an oscilloscope, confirming its linear dependence with applied power.

We thus measure the effective nuclear Rabi frequency as a function of the normalized RF amplitude $B_1/|B_{1,max}|$ in all three electronic manifolds (Fig. 4). The measured Rabi frequency Ω_m is related to its on-resonance value by $\Omega_m = \sqrt{\Omega^2 + \delta^2}$, where δ is the detuning from the nuclear spin resonance frequency. We incorporate this unknown, small detuning in our model and fit the experimental data with the Rabi enhancement formulas (5-7). From the fit, we obtain an estimate of the transverse hyperfine coupling, $A_{\perp} = -2.62 \pm 0.05$ MHz, in good agreement with recently published values and with better precision than previously measured.

In order to achieve even better precision, we need to consider all the sources of uncertainty and errors. We find that small errors from imperfect MW π pulses and nuclear polarization only contribute to a reduced fluorescent contrast, but do not affect the estimate of the Rabi frequency under our experimental condition. The detuning of the selective MW and RF pulses from resonance and uncertainty in A_{\parallel} contributes only linearly to the uncertainty. All these minor errors and uncertainties affect very little the final uncertainty in the estimate of A_{\perp} ³⁴. The major source of error arises instead from the uncertainty in the measured Rabi frequency, which is limited by photon shot noise of the optical read-out process. Therefore, the precision of the estimate could be improved with more averaging, at the expense of longer measurement time. Currently our total measurement time is limited by the stability of experimental setup, yielding $\delta A_{\perp} \sim 50$ kHz. Improving the stability of the setup by reducing thermal fluctuations and noise in the driving field (also using decoupling schemes^{36,37}) or

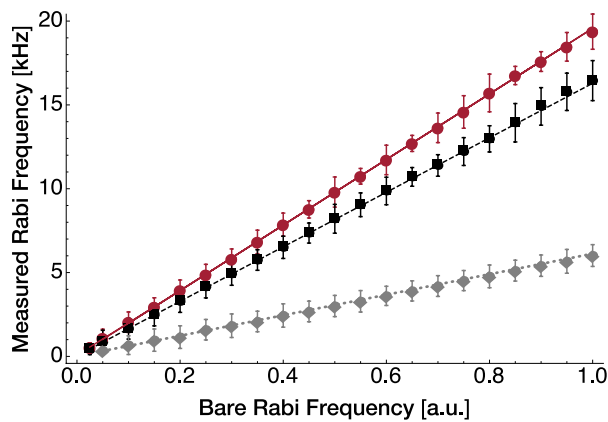


FIG. 4. Measured enhanced ^{14}N Rabi Frequency in the three NV manifold (Red, solid line $m_s = 0$. Black, dashed line, $m_s = -1$. Gray, dotted line $m_s = +1$) as a function of the bare Rabi frequency at $B = 509\text{G}$.

employing small ensembles or more efficient optical read-out methods such as solid-immersion lenses³⁸ and charge-state sensing³⁹ could provide higher precision. Then, the

limit would come from uncertainties in γ_e and γ_n , with relative error of $10^{-426,40}$, yielding an uncertainty in A_{\perp} of a few hundred Hz³⁴.

Conclusions – In conclusion, we observed enhanced nuclear Rabi oscillation in the NV- ^{14}N system due to level mixing between electronic and nuclear spin states. We harness the strong dependence of this enhancement on the transverse hyperfine coupling to determine its value with higher precision than previously published results. Theoretical analysis predicts an enhancement factor of almost 3 orders of magnitude when the magnetic field is close to the ground state level anti-crossing, promising fast manipulation of nuclear spin qubit at $\sim \text{MHz}$ rates, with only moderate driving strengths. More broadly, the method presented here can be applied to many other electron-nuclear hybrid spin systems to similarly characterize their interaction Hamiltonian with high precisions. Our results indicate that taking into account non-secular parts of a system’s Hamiltonian is crucial to achieving faster and more accurate control of the quantum system.

Acknowledgements – This work was supported in part by the U.S. Air Force Office of Scientific Research grant No. FA9550-12-1-0292 and by the U.S. Office for Naval Research grant No. N00014-14-1-0804.

* These authors contributed equally to this work.

† pcappell@mit.edu

¹ N. Khaneja, T. Reiss, C. Kehlet, T. Schulte-Herbuggen, and S. Glaser, *J. Magn. Res.* **172**, 296 (2005).

² J. Scheuer, X. Kong, R. S. Said, J. Chen, A. Kurz, L. Marsiglia, J. Du, P. R. Hemmer, S. Montangero, T. Calarco, B. Naydenov, and F. Jelezko, *New J. Phys.* **16**, 093022 (2014).

³ A. Gruber, A. Drabenstedt, C. Tietz, L. Fleury, J. Wrachtrup, and C. v. Borczyskowski, *Science* **276**, 2012 (1997).

⁴ A. Abragam and B. Bleaney, *Electron Paramagnetic Resonance of Transition Ions* (Clarendon Press, Oxford, 1970).

⁵ S. Sangtawesin and J. R. Petta, “Hyperfine-enhanced gyromagnetic ratio of a nuclear spin in diamond,” (2015), arXiv:1503.07464.

⁶ J. E. Field, ed., *The Properties of Natural and Synthetic Diamond* (Academic Press, London, 1992).

⁷ J. M. Taylor, P. Cappellaro, L. Childress, L. Jiang, D. Budker, P. R. Hemmer, A. Yacoby, R. Walsworth, and M. D. Lukin, *Nat. Phys.* **4**, 810 (2008).

⁸ F. Dolde, H. Fedder, M. W. Doherty, T. Nobauer, F. Rempp, G. Balasubramanian, T. Wolf, F. Reinhard, L. C. L. Hollenberg, F. Jelezko, and J. Wrachtrup, *Nat. Phys.* **7**, 459 (2011).

⁹ D. M. Toyli, C. F. de las Casas, D. J. Christle, V. V. Dobrovitski, and D. D. Awschalom, *Proc. Nat. Acad. Sci.* **110**, 8417 (2013).

¹⁰ J. Wrachtrup, S. Kilin, and A. Nizovtsev, *Optics and Spectroscopy* **91**, 429 (2001).

¹¹ P. Cappellaro, L. Jiang, J. S. Hodges, and M. D. Lukin, *Phys. Rev. Lett.* **102**, 210502 (2009).

¹² I. Aharonovich, A. D. Greentree, and S. Prawer, *Nature Photonics* **5**, 397 (2011).

¹³ B. J. M. Hausmann, B. Shields, Q. Quan, P. Maletinsky, M. McCutcheon, J. T. Choy, T. M. Babinec, A. Kubanek, A. Yacoby, M. D. Lukin, and M. Loncar, *Nano Letters* **12**, 1578 (2012).

¹⁴ G. D. Fuchs, G. Burkard, P. V. Klimov, and D. D. Awschalom, *Nat. Phys.* **7**, 789 (2011).

¹⁵ G. Waldherr, P. Neumann, S. F. Huelga, F. Jelezko, and J. Wrachtrup, *Phys. Rev. Lett.* **107**, 090401 (2011).

¹⁶ R. E. George, L. M. Robledo, O. J. E. Maroney, M. S. Blok, H. Bernien, M. L. Markham, D. J. Twitchen, J. J. L. Morton, G. A. D. Briggs, and R. Hanson, *Proc. Nat. Acad. Sci.* **110**, 3777 (2013).

¹⁷ P. Neumann, J. Beck, M. Steiner, F. Rempp, H. Fedder, P. R. Hemmer, J. Wrachtrup, and F. Jelezko, *Science* **5991**, 542 (2010).

¹⁸ E. M. Kessler, I. Lovchinsky, A. O. Sushkov, and M. D. Lukin, *Phys. Rev. Lett.* **112**, 150802 (2014).

¹⁹ G. Arrad, Y. Vinkler, D. Aharonov, and A. Retzker, *Phys. Rev. Lett.* **112**, 150801 (2014).

²⁰ M. P. Ledbetter, K. Jensen, R. Fischer, A. Jarmola, and D. Budker, *Phys. Rev. A* **86**, 052116 (2012).

²¹ A. Ajoy and P. Cappellaro, *Phys. Rev. A* **86**, 062104 (2012).

²² M. Steiner, P. Neumann, J. Beck, F. Jelezko, and J. Wrachtrup, *Phys. Rev. B* **81**, 035205 (2010).

²³ B. Smeltzer, J. McIntyre, and L. Childress, *Phys. Rev. A* **80**, 050302 (2009).

²⁴ C. S. Shin, M. C. Butler, H.-J. Wang, C. E. Avalos, S. J. Seltzer, R.-B. Liu, A. Pines, and V. S. Bajaj, *Phys. Rev. B* **89**, 205202 (2014).

- ²⁵ J. G. Kempf and D. P. Weitekamp, *Journal of Vacuum Science & Technology B* **18**, 2255 (2000).
- ²⁶ M. W. Doherty, N. B. Manson, P. Delaney, F. Jelezko, J. Wrachtrup, and L. C. Hollenberg, *Physics Reports* **528**, 1 (2013).
- ²⁷ S. Felton, A. M. Edmonds, M. E. Newton, P. M. Martineau, D. Fisher, D. J. Twitchen, and J. M. Baker, *Phys. Rev. B* **79**, 075203 (2009).
- ²⁸ X.-F. He, N. B. Manson, and P. T. H. Fisk, *Phys. Rev. B* **47**, 8816 (1993).
- ²⁹ J. J. L. Morton, A. M. Tyryshkin, R. M. Brown, S. Shankar, B. W. Lovett, A. Ardavan, T. Schenkel, E. E. Haller, J. W. Ager, and S. A. Lyon, *Nature* **455**, 1085 (2008).
- ³⁰ G. Wolfowicz, M. Urdampilleta, M. L. W. Thewalt, H. Riemann, N. V. Abrosimov, P. Becker, H.-J. Pohl, and J. J. L. Morton, *Phys. Rev. Lett.* **113**, 157601 (2014).
- ³¹ M. Widmann, S.-Y. Lee, T. Rendler, N. T. Son, H. Fedder, S. Paik, L.-P. Yang, N. Zhao, S. Yang, I. Booker, A. Denisenko, M. Jamali, S. A. Momenzadeh, I. Gerhardt, T. Ohshima, A. Gali, E. Janzén, and J. Wrachtrup, *Nature Mat.* **14**, 164 (2015).
- ³² A. L. Falk, P. V. Klimov, V. Ivády, K. Szász, D. J. Christle, W. F. Koehl, Á. Gali, and D. D. Awschalom, “Optical polarization of nuclear spins in silicon carbide,” (2015).
- ³³ E. A. Chekhovich, M. N. Makhonin, A. I. Tartakovskii, A. Yacoby, H. Bluhm, K. C. Nowack, and L. M. K. Vandersypen, *Nature Mat.* **12**, 494 (2013).
- ³⁴ See Supplemental Material at [URL will be inserted by publisher] for technical details of theoretical model and error analysis.
- ³⁵ V. Jacques, P. Neumann, J. Beck, M. Markham, D. Twitchen, J. Meijer, F. Kaiser, G. Balasubramanian, F. Jelezko, and J. Wrachtrup, *Phys. Rev. Lett.* **102**, 057403 (2009).
- ³⁶ J.-M. Cai, B. Naydenov, R. Pfeiffer, L. P. McGuinness, K. D. Jahnke, F. Jelezko, M. B. Plenio, and A. Retzker, *New J. Phys.* **14**, 113023 (2012).
- ³⁷ C. D. Aiello, M. Hirose, and P. Cappellaro, *Nat. Commun.* **4**, 1419 (2013).
- ³⁸ L. Marseglia, J. P. Hadden, A. C. Stanley-Clarke, J. P. Harrison, B. Patton, Y.-L. D. Ho, B. Naydenov, F. Jelezko, J. Meijer, P. Dolan, J. Smith, J. Rarity, and J. O'Brien, *Appl. Phys. Lett.* **98**, 133107 (2011).
- ³⁹ B. J. Shields, Q. P. Unterreithmeier, N. P. de Leon, H. Park, and M. D. Lukin, *Phys. Rev. Lett.* **114**, 136402 (2015).
- ⁴⁰ P. Neumann, *Towards a room temperature solid state quantum processor—The nitrogen-vacancy center in diamond*, Ph.D. thesis, University of Stuttgart (2012).